

RESEARCH ARTICLE

 OPEN ACCESS

Received: 13-12-2023

Accepted: 04-02-2024

Published: 23-02-2024

Citation: Gore AS, Patil NG, Farooqui MN (2024) Mathematical Modeling and Finite Element Analysis of Wire Electro-Discharge Machining of Ceramic Particulate Reinforced Metal Matrix Composite Material. Indian Journal of Science and Technology 17(9): 852-862. <https://doi.org/10.17485/IJST/v17i9.3131>

* **Corresponding author.**goreabhay13@gmail.com**Funding:** None**Competing Interests:** None

Copyright: © 2024 Gore et al. This is an open access article distributed under the terms of the [Creative Commons Attribution License](https://creativecommons.org/licenses/by/4.0/), which permits unrestricted use, distribution, and reproduction in any medium, provided the original author and source are credited.

Published By Indian Society for Education and Environment ([iSee](https://www.isee.org/))

ISSN

Print: 0974-6846

Electronic: 0974-5645

Mathematical Modeling and Finite Element Analysis of Wire Electro-Discharge Machining of Ceramic Particulate Reinforced Metal Matrix Composite Material

Abhay S Gore^{1*}, Nilesh G Patil², Mohammed Naser Farooqui³

¹ Research Scholar, Department of Mechanical Engineering, Maharashtra Institute of Technology, Chh. Sambhajinagar, Maharashtra, India

² Director, Department of Mechanical Engineering, Maharashtra Institute of Technology, Chh. Sambhajinagar, Maharashtra, India

³ Assistant Professor, Department of Mechanical Engineering, Maharashtra Institute of Technology, Chh. Sambhajinagar, Maharashtra, India

Abstract

Objectives: A mathematical model is formulated for WEDM process for machining of Al/SiC/p to predict crater size, material removal rate for single spark discharge and same model is extended for multiple spark discharges which is not extensively studied in the literature. This was done by considering previous experimental data from the literature. **Methods:** A mathematical model predicts heat flux, radius of crater, material removal rate. Mode of heat transfer considered as conduction through workpiece. Material modeling is done considering the number of reinforced particles in the given volume. For random distribution of reinforced particles, a code is written in MATLAB software tool. Co-ordinates of these reinforced particles are extracted for FEA simulation in ABAQUS software tool. Material properties are considered as temperature dependent. This methodology is not adopted for MMCs. **Findings:** Results of theoretical model, FEA simulation and experimentation are compared. The predicted MRR by FEA simulation is 2% error at lower Ton values as $0.2\mu\text{s}$ and $0.4\mu\text{s}$ to that of experimental MRR. **Novelty:** Crater size becomes shallow with increase in volume percentage of SiC particles resulting greater crater radius. With increased pulse on time MRR increases up to certain limit and then decreases.

Keywords: WEDM; Modeling; MMC; FEA; MRR

1 Introduction

Material selection in engineering often presents a challenging decision-making process characterized by a paradox. It can be a daunting task to find a single material that possesses all the necessary properties for a given application. Lightweight materials, for

instance, tend to lack the required strength, while brittle materials often fall short in terms of stiffness, toughness, and fatigue resistance. This inherent contradiction makes the pursuit of the ideal material choice a complex and intricate endeavor⁽¹⁾. A composite material is essentially a combination of two or more phases that are chemically distinct at a microscopic level, and they are visibly distinguishable. Within this composite structure, one component, known as the matrix, typically comprises a larger proportion. The expectation when creating a composite is that it will lead to an enhancement of the material's properties. The second part of this composite is referred to as the reinforcement, and its role is to enhance or strengthen the mechanical characteristics of the matrix. This synergy between the matrix and the reinforcement is key to achieving improved overall performance in composite materials⁽²⁾. Aluminum matrix composites (AMCs) are associated with several challenges that render traditional processing methods impractical. These challenges include increased energy consumption, elevated equipment costs, poor machinability, subpar surface quality, and substantial wear and tear on cutting tools. These factors collectively make it a less viable option to employ conventional processing techniques for AMCs⁽³⁾. Aluminum matrix composites (AMCs) represent unconventional lightweight metals that offer a unique combination of advantageous properties, including excellent wear resistance, high strength, and low thermal expansion. These attributes make AMCs a popular choice across various industrial applications⁽⁴⁾. The hardness and the presence of reinforcement in metal matrix composites (MMCs) pose significant challenges when attempting to machine them using traditional techniques. This is especially pronounced when there is a requirement for creating precise parts and intricate shapes. These challenges have acted as a deterrent and hindered the swift advancement of MMCs in certain applications⁽⁵⁾. The Al/SiC/10%, Al/SiC/20% and Al/SiC/30% are considered for the same reason. While the addition of aluminum reinforcement enhances the overall characteristics of the composite, it also increases its hardness, rendering machining a highly challenging task. While it is possible to address this challenge by employing advanced machining processes such as water jet cutting and laser-based machining, it's worth noting that the machinery required for these processes can be expensive, and there may be limitations on the workpiece height, which can impact the feasibility of such solutions⁽⁶⁾. As a result, there is a pressing need for efficient cutting methods that can deliver both superior surface quality and maintain precision in the machining of such materials⁽⁷⁾. Hence, Wire EDM (Electrical Discharge Machining) emerges as the preferred choice for machining composites, as it excels in handling intricate and complex shapes, offering a high level of control and precision in the process. An unconventional machining method like Electrical Discharge Machining (EDM) can be a suitable choice. It operates by intermittently generating electrical sparks to remove particles from the material's surface. In contrast to traditional procedures that rely on abrasion for material removal, EDM does not involve direct physical contact between the tool and the workpiece, which means that tool wear is significantly reduced in Wire EDM (WEDM)⁽⁸⁾. In EDM, both the tool and the workpiece act as electrodes, facilitating the material removal process. The tool is typically made of a harder material than the workpiece to effectively remove material. However, it is important to note that the operation costs in EDM tend to be high because this method involves a relatively longer machining time through surface erosion⁽⁹⁾. The peak current, pulse on time, pulse off time, wire feed, wire tension, and voltage are the input parameters that have the most impact on WEDM machining. Out of these input parameters pulse-on-time had the most significant effect on MRR, pulse-peak current and pulse-off-time are also noticed to be statistically significant effect⁽¹⁰⁾. A mathematical model has been developed for the Wire Electrical Discharge Machining (WEDM) process, specifically for machining Al/SiC/p composites, focusing initially on single spark discharge. This model is then expanded to account for multiple spark discharges by taking into consideration the relevant experimental data provided in literature, Patil et al.⁽¹¹⁾. This will shed a fundamental insight on the principle working mechanism of Wire EDM process using more realistic assumptions being in line with the true nature of Wire EDM. These mainly involve the Gaussian distribution of heat flux, spark radius, temperature-dependent material properties, and the fraction of discharge energy entering the workpiece. Study of crater morphology obtained through simulations and comparing with experimental results. This offers a distinct foundation for assessing and contrasting the current model's predicted accuracy with alternative methods in relation to the results of the experiment.

2 Methodology

The proposed model utilizes Gaussian distribution as a heat source, Fourier heat conduction equation as governing equation, temperature dependent material properties of matrix as well as reinforced particles, this leads to prediction of heat flux, spark radius and MRR. For material modeling random distribution of reinforced particles in matrix is done unlike homogeneous distribution⁽¹²⁾. Available models from literature are for conventional materials⁽¹³⁾, which makes proposed methodology unique, more realistic, and accurate.

2.1 Process Modeling

A Model has been developed considering Gaussian heat source⁽¹⁴⁾ with following assumptions made

Assumptions

1. Small volume of material removed per each discharge compared to workpiece and tool electrodes' volumes, semi-infinite bodies are considered for the workpiece and tool.
2. The domain for thermal analysis is assumed to be 2D to reduce computational time.
3. One spark happens during each pulse.
4. A constant fraction of spark thermal energy is transferred to the workpiece by conduction, the rest is used for tool wear as well as dissipation via convection and radiation through the dielectric medium.
5. Conduction is the main mode of heat transfer from the spark channel to the workpiece surface as the contribution of other mechanisms such as convection and radiation is neglected.
6. The workpiece is assumed to be homogeneous and isotropic while its thermo-physical properties are considered as temperature dependent.
7. All the materials whose temperature exceeds the melting temperature are assumed to be effectively removed by the dielectric flushing upon the collapse of plasma channel, so there is no deposition of recast layer at the bottom of crater cavity formed at the end of each discharge.
8. The initial temperature was set to room temperature.

2.1.1 Heat Source

Various models like Gaussian distribution, uniform disc heat source models exist. Of them Gaussian distribution has proven to be accurate to the experimental results shown in Figure 1.

The heat source is assumed to have a Gaussian distribution of heat flux on the surface of the workpiece.

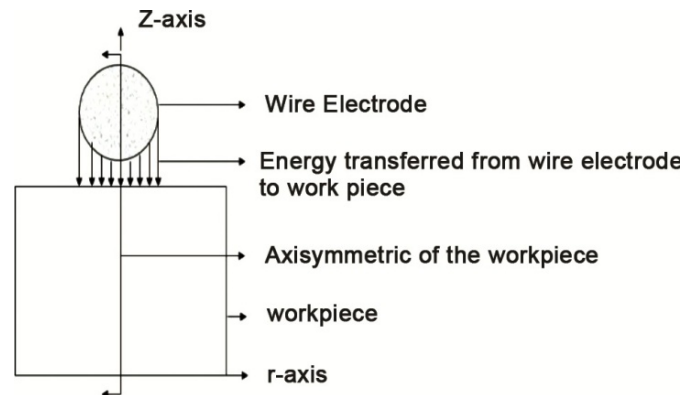


Fig 1. Thermal model of WEDM

2.1.2 Governing Equation

Conduction has been considered as the main mode of heat transfer in WEDM, Therefore the Fourier heat conduction equation has been solved for the analysis of thermal modeling with no internal heat generation in cylindrical coordinates.

$$\frac{1}{\alpha} \frac{\partial T}{\partial t} = \frac{\partial^2 T}{\partial r^2} + \frac{1}{r} \frac{\partial T}{\partial r} + \frac{1}{r^2} \frac{\partial^2 T}{\partial \phi^2} + \frac{\partial^2 T}{\partial z^2} \quad (1)$$

where, T is temperature of the work- piece (K), r, z and ϕ are coordinate axes and t is time for the spark (μ s). α is the thermal diffusivity which can be represented as,

$$\alpha = \frac{K_t}{\rho C_p}$$

Heating of a workpiece is due to single spark which is assumed to be axisymmetric so,

$\frac{\partial T}{\partial \phi} = 0$, thus Equation (1) becomes,

$$\frac{1}{\infty} \frac{\partial T}{\partial t} = \frac{\partial^2 T}{\partial r^2} + \frac{1}{r} \frac{\partial T}{\partial r} + \frac{\partial^2 T}{\partial z^2} \tag{2}$$

$$\rho c \frac{\partial T}{\partial t} = \frac{1}{r} \frac{\partial}{\partial r} \left(k \frac{\partial T}{\partial r} \right) + \frac{\partial}{\partial z} \left(k \frac{\partial T}{\partial z} \right) \tag{3}$$

Where, k is thermal conductivity of the workpiece (W/mK), ρ is density of the workpiece (kg/m³), c is specific heat of the workpiece (J/kg K).

2.1.3 Boundary conditions

The following are the boundary conditions taken for the analysis shown in Figure 2.

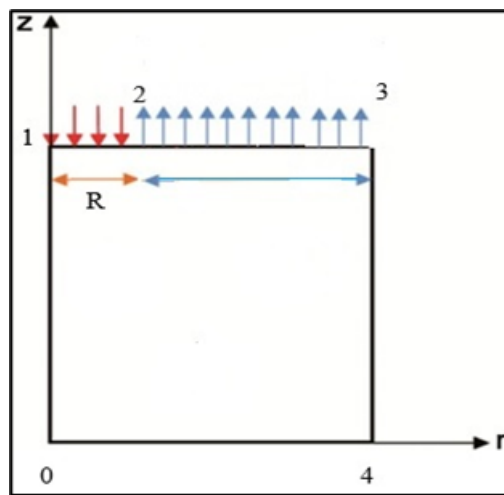


Fig 2. Boundary Condition

The workpiece domain 0-1-3-4 is considered as axisymmetric at 0-1. The heat input point will be at 1, which is maximum. On the top surfaces 1-2, the heat transferred to the workpiece is shown by Gaussian heat flux distribution. Heat flux is applied on boundary 1-2 up to spark radius R, beyond R convection takes place due to dielectric fluids. As 3-4 and 4-0 are far from the spark location no heat transfer conditions have been assumed for them. For boundary 0-4, as it is axis of symmetry the heat transfer is zero. In mathematical terms, the applied boundary conditions are given as follows:

$k \frac{\partial T}{\partial z} = Q(r)$, when $R < r$ for boundary 1-3

$k \frac{\partial T}{\partial z} = h_f(T - T_0)$, when $R \geq r$ for boundary 1-3

$\frac{\partial T}{\partial n} = 0$, at boundary 3-4,4-0,0-1

Where h_f is heat transfer coefficient of dielectric fluid, $Q(r)$ is heat flux due to the spark and T_0 is the initial temperature.

2.1.4 Material properties

Material of workpiece- A356/SiC_p/10% is used.

The temperature dependent material properties of matrix and reinforcement are given in Table 1 and Table 2 respectively.

Table 1. Material properties of A356

Sr. No.	T (K)	ρ (kg/m ³)	C (kJ/kg K)	K (W/m K)
1	150	2726	0.683	250
2	200	2719	0.797	237
3	250	2710	0.859	235

Continued on next page

Table 1 continued

4	300	2701	0.902	237
5	400	2681	0.949	240
6	600	2639	1.042	231

Table 2. Material properties of SiC Alpha

Sr. No.	T (K)	ρ (kg/m ³)	C (J/kg K)	K (W/m K)
1	293	3160	715	114
2	773	3140	1086	55.1
3	1273	3110	1240	35.7
4	1473	3100	1282	31.3
5	1673	3090	1318	27.8
6	1773	3080	1336	26.3

Along with these properties, Latent heat, Solidus temperature, Liquidus temperature for A356 of 396000 KJ/Kg, 830 K, 886 K and SiC Alpha 350000 KJ/Kg, 2973 K, 3130 K considered, respectively.

2.1.5 Heat Source

A Gaussian distribution for heat flux is assumed in this analysis. The governing equation is

$$Q(r) = \frac{4.45VIf}{\pi R^2} e^{-4.5\left(\frac{r}{R}\right)^2} \tag{4}$$

where V is the discharge voltage, I is the current, f is the percentage heat input to the workpiece, and R is the spark radius.

2.1.6 Spark Radius

A Semi-empirical equation of spark radius termed as Equivalent heat input radius is used.

$$R = 2.04e^{-3} I^{0.43} t_{on}^{0.44} \tag{5}$$

2.1.7 Material Removal Rate

Crater morphology predicts the MRR. As heat source considered as Gaussian heat source, crater morphology is spherical⁽¹³⁾. This is shown in Figure 3.

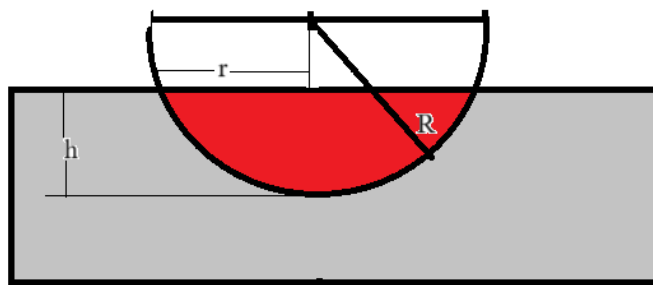


Fig 3. Crater morphology

Where r is the radius and h is depth of spherical dome. The volume of spherical dome can be calculated to find out volume of material removal in single discharge.

$$C_v = \frac{1}{6} \pi h(3r^2 + h^2) \tag{6}$$

The Number of Pulses can be calculated by dividing the total machining time to pulse duration as given,

$$NOP = \frac{T_{mach}}{T_{on} + T_{off}} \quad (7)$$

Where, T_{mach} is machining time, T_{on} is pulse on time and T_{off} is pulse off time.

MRR for multiple discharge can be found as

$$MRR = \frac{C_v * NOP}{T_{mach}} \quad (8)$$

2.2 Material Modeling

Representative volume modeling is adapted to model the material. Particles of ceramic reinforcement are randomly distributed in aluminum matrix, as manufacturing process is stir casting. Number of particles per in given volume can be found by using Rule of mixture,

$$V_f = \frac{4N\pi D^3}{24LWH} \quad (9)$$

Where,

V_f = Volume fraction

N= Number of particles

D= Diameter of particle

L= Length of volume

W= Width of volume

H= Height of volume

Equation can be rewritten to find number of particles in a volume as

$$N = \frac{24LWHV_f}{4N\pi D^3} \quad (10)$$

Assume dimension of volume as $50 \mu\text{m}$, the number of particles will be 14.

2.2.1 Material Modeling using MATLAB

A code is written in MATLAB for random distribution of particles and extract center points for further CAD modeling.

The following are assumptions considered.

1. Particles are randomly distributed in the given volume.
2. Particles are non-overlapping.
3. Particles are of uniform diameter.
4. Gap between each particle is maintained as twice the radius.
5. Particles are allowed on surfaces.

As 3D model shown in Figure 4 a) require much more computational resources so the model is simplified in to 2D space shown in Figure 4 b) and center points are extracted from this model, which will be used for CAD modeling.

2.2.2 Finite Element Analysis

ABAQUS software tool is used to carry out CAD modeling and FEA analysis. For 3D modeling volume is extruded and particles are rotated. Particles are trimmed on the surface. Material properties are assigned as specified in Tables 1 and 2. Heat flux is considered as input which is applied over time step as pulse on time i.e., heating time and heat transfer through conduction as pulse off time i.e., cooling time. Output is considered as temperature distribution and heat flux magnitude [Figure 5 a), b)].

The temperature of elements exceeding the melting temperature of material are removed through melting and evaporation^(15,16). This shows the crater morphology to find out the MRR [Figure 5c)].

From the temperature distribution, it is evident that the temperature rises during pulse on time. This temperature rise is sufficient to melt the matrix due to its low melting point. But the reinforced particles remain in particle form due to high

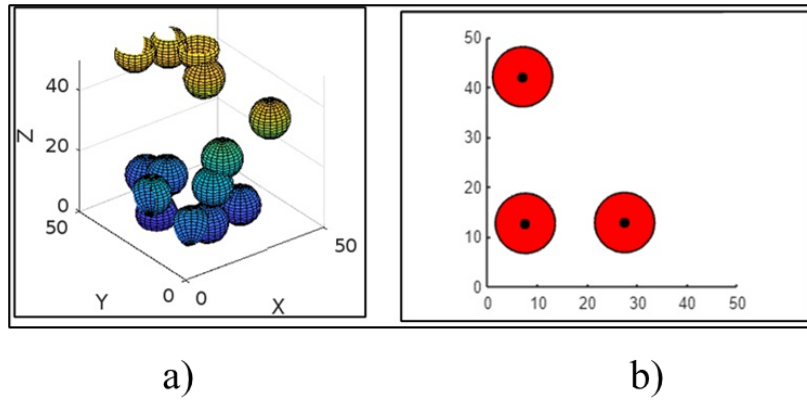


Fig 4. Random distribution of particles in space: a) 3D space, b) 2D space

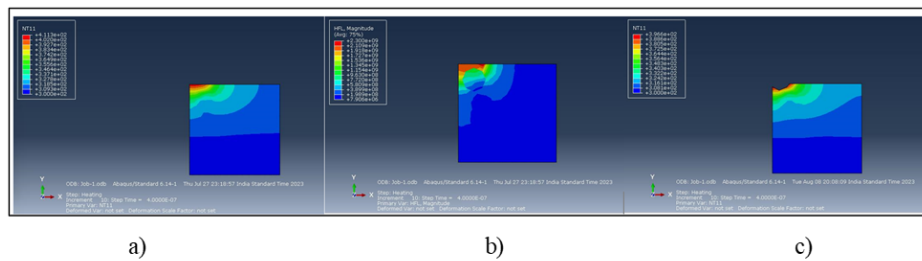


Fig 5. Output of ABAQUS: a) Temperature distribution, b) Heat flux magnitude, c) Crater morphology

melting point. As matrix melts particles lose bonding resulting in greater crater size and thus increased MRR. This stage is a heating stage and mode of heat transfer by conduction mode⁽¹⁵⁾.

During pulse off time, spark does not exist between electrodes. So, no heat flux applied on the workpiece. This stage is cooling stage and mode of heat transfer is convection in dielectric.

The initial temperature of the system is considered at room temperature. But after initial discharge considerable increase in temperature is observed after cooling stage also.

This is a particularly important phenomenon in analysis during multiple discharges⁽¹⁵⁾.

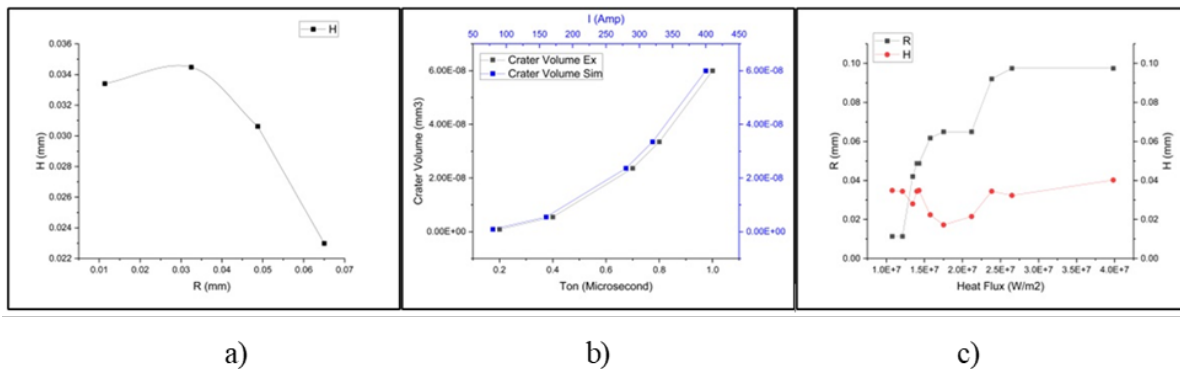


Fig 6. Crater analysis: a) Heat flux vs R, H, b) Crater radius vs crater height, c) Ton, Current vs crater volume

As heat flux increases, crater volume supposed to be increased. SiC particles have lower thermal conductivity compared to Al matrix. This results into restriction of heat transfer along height and increase of heat transfer in radial direction. So, there is

increase in radius of crater and decrease in height of crater resulting shallow crater.

This phenomenon is more significant in higher values of heat flux. At higher values of heat flux radius of crater tends to be increased and height of crater gradually decreases.

Ton and current are main factors that controls the heat flux⁽¹⁷⁾. Figure 6 shows the relationship between Ton, current and experimental and simulated crater volumes. Though, crater is getting shallower, the experimental and simulated MRR are almost same. Simulated crater volume is higher than that of experimental because of neglected dielectric media, and unpredicted machining conditions.

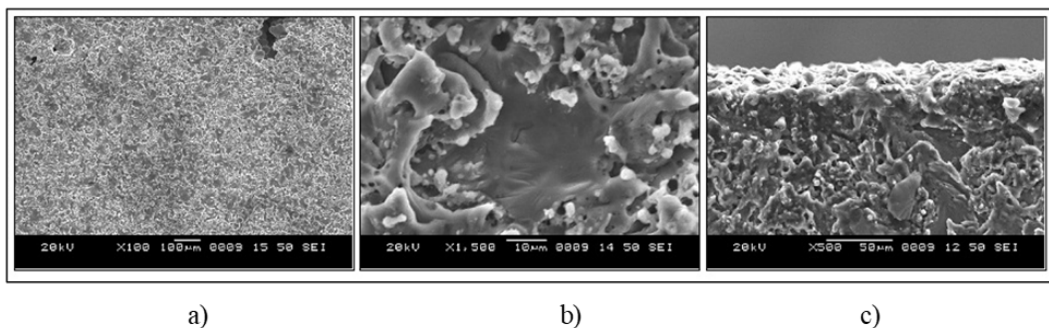


Fig 7. Surface morphology: a) Reinforced Particles, b) Dislodged reinforced particle, c) Recast layer

Figure 7a)⁽¹¹⁾ shows presence of reinforced SiC particles. During machining heat is transferred to workpiece by conduction mode and some heat dissipate to dielectric media. Due to huge amount of heat flux induced Al matrix starts melting as lower melting point compared to reinforced SiC particles, but reinforced SiC particles have high melting point so these particles don't melt. The Al matrix around SiC particles melt and flushed leaving particles to dislodge^(16,17), this can be seen in Figure 7b). The material that has been over-melted but not completely removed is accounted for by the recast layer⁽¹⁷⁾. Figure 7 c) shows recast layer. Same phenomenon is observed for FEA results. Figure 7 b) shows similarity regarding melting of matrix around particles, resulting dislodging.

3 Results and Discussion

In previous section, crater morphology is analysed. Heat flux is dependent on input parameters as Ton, Toff, voltage and current. The geometrical shape of crater tends to be shallower as values of heat flux increased. Crater shape decides the MRR. MRR are compared for experimental values, theoretical values, and simulated values as shown in Figure 8.

There is proportional increase in MRR from Ton=0.2 Toff=12, V=40, I=100, Figure 8 a) up to Ton=0.4, Toff=14, V=40, I=155, Figure 8 b). After that MRR increased from Ton=0.7, Toff=14 V=45, I=260, Figure 8 c). And MRR increased rapidly from Ton=0.8, Toff=14 V=45, I= 320, Figure 8 d). Pulse on time influence the heat flux and ultimately MRR. MRR values of theoretical is grater compared to that of simulated and experimental, the reason could be only conduction mode of heat transfer is considered. In actual the energy that is delivered to the workpiece by the plasma channel is divided into three parts. One is used to heat up the workpiece, while the other part is conducted into the workpiece, and some dissipate to the dielectric media⁽¹⁶⁾.

MRR of Al/SiCp/10% composites for experimental and simulated shows good co-relationship from Ton=0.2 to Ton=0.7. After that simulated MRR slightly differs than experimental MRR up to Ton=1. Al/SiCp/10% contains less SiC particles thus heat flux applied to workpiece results into good crater radius and depth. Figure 9 a) justifies the same.

In Al/SiC/20% composites experimental and simulated MRR follows the same curve, simulated shows good results at Ton=0.2 after that its slightly higher this might be because of convection heat transfer not considered. At Ton=0.7, experimental MRR is less than simulated. In Al/SiC/20% composites number of SiC particles are more and these particles have lower thermal conductivity. More heat flux might be utilized to heat up the workpiece so heat might dissipate into dielectric.

For Al/SiC/30% both experimental and simulated MRR are same up to Ton=0.7, beyond that it differs, Figure 9b). This shows Ton is significant factor that decides the MRR. Theoretical and experimental MRR are same when Ton=0.2 for all three composites. The model predicts correct MRR when Ton=0.2, 0.4,0.7 for Al/SiCp/10%, Ton=0.2 for Al/SiCp/20% and Ton=0.2,0.4,0.7 for Al/SiCp/30%, Figure 9 c).

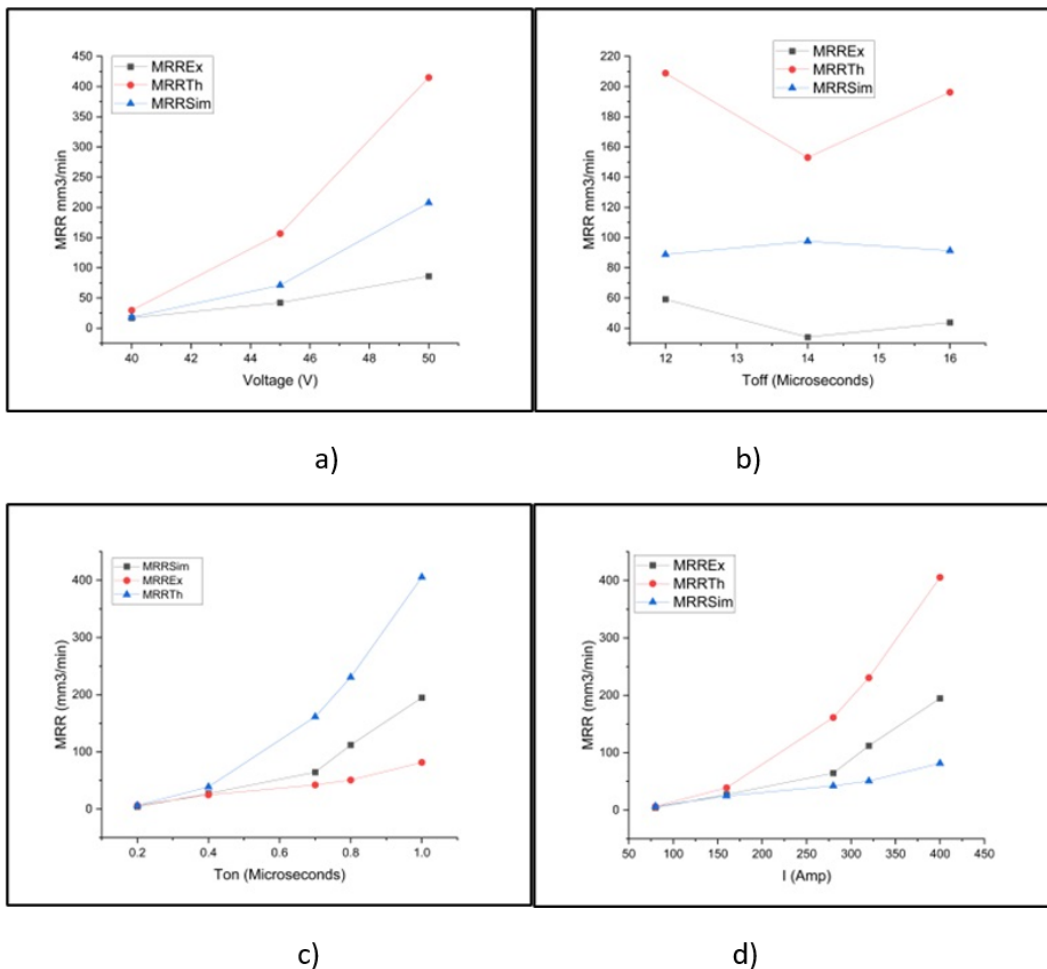


Fig 8. Effect of input parameters on MRR: a) Ton vs MRR, b) Toff vs MRR, c) Voltage vs MRR, d) Current vs MRR

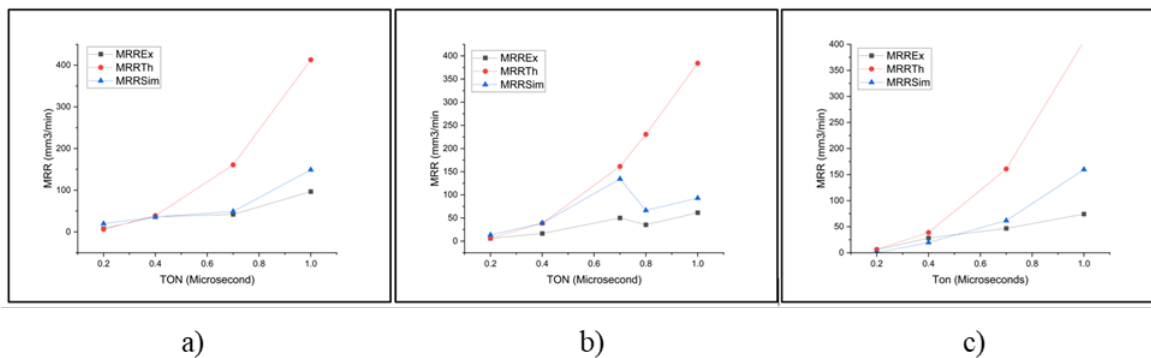


Fig 9. Ton vs MRR: a) Al/SiC/10%, b) Al/SiC/20%, c) Al/SiC/30%

In all three composites, theoretical MRR reinforced SiC particles are not considered, rather than composites it is applicable for homogenous materials. So, there is need to consider percentage of particles for modelling.

Experimental MRR and simulated MRR shows good prediction for all composites. Good co-relation observed at lower SiC content⁽¹⁸⁾ i.e., Al/SiCp/10% composites with 2% error, whereas literature shows 9.3%.⁽¹⁷⁾

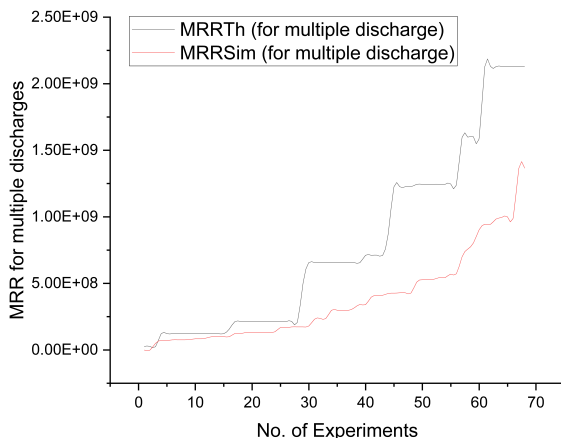


Fig 10. Number of experiments vs MRR

Figure 10 shows MRR for multiple discharges. The model predicts good correlation between experimental and simulated MRR, so model can be extended from single discharge to multiple discharge. For first 30 experiments theoretical and simulated MRR found to be same. After that increasing SiC particles simulated MRR decreasing. Same trend is observed in experimental MRR also.

4 Conclusion

In present study a model has been developed to model the Al/SiC/p, process of WEDM and prediction of the MRR. While modelling of Al/SiC/p rule of mixture, random distribution of SiC particles and the temperature dependent properties are considered. In process modelling of WEDM Gaussian heat source used which is promising. First model is developed for single discharge and then extended for multiple discharges. FEA is carried out to predict the crater morphology which is then compared to theoretical model. This leads to prediction of MRR by theoretical and simulated results. These results are compared with experimental results.

Model predicts good co-relationship with experimental and simulated results for Al/SiC/10% with 2% error. For Al/SiC/20% and Al/SiC/30% MRR predicted for lower values of Ton agrees with experimental MRR. This found to be limited at lower values of pulse on time Ton=0.2. The extended model of multiple discharges was also limited to lower values of Ton i.e. Ton= 0.2 & 0.4. As increase in percentage of SiC particles, simulated MRR decreases as same as experimental and more significant for higher Ton=1. This methodology can be used for other grades of MMCs also. But results may differ at higher percentage of SiC and Ton values.

References

- 1) Ujah CO, Vandi Von Kallon D. Trends in Aluminium Matrix Composite Development. *Crystals*. 2022;12(10):1–27. Available from: <https://doi.org/10.3390/cryst12101357>.
- 2) Razzaq AM, Majid DL, Basheer UM, Aljibori HSS. Research Summary on the Processing, Mechanical and Tribological Properties of Aluminium Matrix Composites as Effected by Fly Ash Reinforcement. *Crystals*. 2021;11(10):1–20. Available from: <https://doi.org/10.3390/cryst11101212>.
- 3) Kumar J, Singh D, Kalsi NS, Sharma S, Mia M, Singh J, et al. Investigation on the mechanical, tribological, morphological and machinability behavior of stir-casted Al/SiC/Mo reinforced MMCs. *Journal of Materials Research and Technology*. 2021;12(May–June):930–946. Available from: <https://doi.org/10.1016/j.jmrt.2021.03.034>.
- 4) Singh H, Brar GS, Kumar H, Aggarwal V. A review on metal matrix composite for automobile applications. *Materials Today: Proceedings*. 2021;43(Part 1):320–325. Available from: <https://doi.org/10.1016/j.matpr.2020.11.670>.

- 5) Bhutta MR, Gillani F, Zahid T, Bibi S, Ghafoor U. Investigation of Hardness and Microanalysis of Sintered Aluminum-Based Supplemented Metal Matrix Machined Composites. *Crystals*. 2023;13(9):1–14. Available from: <https://doi.org/10.3390/cryst13091347>.
- 6) Samal P, Vundavilli PR, Meher A, Mahapatra MM. Recent progress in aluminum metal matrix composites: A review on processing, mechanical and wear properties. *Journal of Manufacturing Processes*. 2020;59:131–152. Available from: <https://doi.org/10.1016/j.jmapro.2020.09.010>.
- 7) Gupta K, Gupta MK. Developments in nonconventional machining for sustainable production: A state-of-the-art review. *Proceedings of the Institution of Mechanical Engineers, Part C: Journal of Mechanical Engineering Science*. 2019;233(12):4213–4232. Available from: <https://doi.org/10.1177/0954406218811982>.
- 8) Thangaraj M, Annamalai R, Moiduddin K, Alkindi M, Ramalingam S, Alghamdi O. Enhancing the Surface Quality of Micro Titanium Alloy Specimen in WEDM Process by Adopting TGRA-Based Optimization. *Materials*. 2020;13(6):1–13. Available from: <https://doi.org/10.3390/ma13061440>.
- 9) Jebarose JS, Udayaprakash J, Ep RC, Karthik K. Multi-Objective Optimization of Machining Parameters for Drilling LM5/ZrO2 Composites Using Grey Relational Analysis. *Materials*. 2023;16(10):1–13. Available from: <https://doi.org/10.3390/ma16103615>.
- 10) Kumar A, Grover N, Manna A, Chohan JS, Kumar R, Singh S, et al. Investigating the influence of WEDM process parameters in machining of hybrid aluminum composites. *Advanced Composites Letters*. 2020;29:1–14. Available from: <https://doi.org/10.1177/2633366X20963137>.
- 11) Patil NG, Brahmanekar PK. Determination of material removal rate in wire electro-discharge machining of metal matrix composites using dimensional analysis. *The International Journal of Advanced Manufacturing Technology*. 2010;51(5-8):599–610. Available from: <https://doi.org/10.1007/s00170-010-2633-3>.
- 12) Ahmadiania OF, Küçüktürk G, Sucularlı F, Gürün H. Machinability of B4C-reinforced Al2014 metal matrix composites in electric discharge machining. *Revista de Metalurgia*. 2022;58(4):1–8. Available from: <https://doi.org/10.3989/revmetalm.228>.
- 13) Taj SN, Shamim FA, Ashraf M, Ali ZAH, Hasan F. Material removal rate prediction for electro discharge machining: Analytical modelling. *Materials Today: Proceedings*. 2023. Available from: <https://doi.org/10.1016/j.matpr.2023.09.186>.
- 14) Chaudhury P, Samantaray S. Finite Element Modelling of EDM of Aluminum Particulate Metal Matrix Composites Considering Temperature Dependent Properties. *Revue des composites et des matériaux avancés*. 2019;29(1):53–62. Available from: <https://doi.org/10.18280/rcma.290109>.
- 15) Li Q, Yang X. Modelling and simulation of surface formation in electrical discharge machining based on thermo-hydraulic coupling. *Precision Engineering*. 2024;85:126–135. Available from: <https://doi.org/10.1016/j.precisioneng.2023.09.013>.
- 16) Zhang W, Chang H, Liu Y. Study on Solidification Process and Residual Stress of SiCp/Al Composites in EDM. *Micromachines*. 2022;13(6):1–16. Available from: <https://doi.org/10.3390/mi13060972>.
- 17) Ram HS, Uthayakumar M, Kumar SS, Kumaran ST, Korniejenko K. Modelling Approach for the Prediction of Machinability in Al6061 Composites by Electrical Discharge Machining. *Applied Sciences*. 2022;12(5):1–25. Available from: <https://doi.org/10.3390/app12052673>.
- 18) Yan YF, Kou SQ, Yang HY, Shu SL, Qiu F, Jiang QC, et al. Ceramic particles reinforced copper matrix composites manufactured by advanced powder metallurgy: preparation, performance, and mechanisms. *International Journal of Extreme Manufacturing*. 2023;5(3):1–35. Available from: <https://iopscience.iop.org/article/10.1088/2631-7990/acdb0b>.